

Measurements in Separating Boundary Layers

M. Dianat* and I. P. Castro†

University of Surrey, Guildford, England, United Kingdom

In this paper we describe the application of pulsed-wire anemometry to the study of a two-dimensional separated flow generated by imposing a suitably adverse pressure gradient on a flat plate turbulent boundary layer. Accurate measurements of both mean velocity right down to the wall and skin friction have been made throughout the region approaching separation and within the separated region itself. The presentation includes a brief description of the development of the specially designed velocity probe, which can be traversed through the wall and enables measurements to be made throughout the viscous dominated wall region. The data obtained within the separated boundary layer are compared briefly with the results of previous studies; in particular, the similarities and differences between shear layers bounding highly turbulent separated regions and the classic plane mixing layer are briefly discussed.

I. Introduction

THE motivation for the present experiments has been to obtain a greater understanding of separated boundary-layer flows. Perhaps the best known and best attested data for a flow of this sort are those of Simpson et al.¹ They used laser anemometry and were able to obtain reasonably accurate velocity and turbulence measurements throughout the whole flow, including the separated region itself. However, Simpson had no means of making skin-friction measurements in this latter part of the flow, and so it is difficult to use the data to investigate the possibility of universal velocity profile shapes in the viscosity-affected region near the wall. The basic objective of the present work was, therefore, to measure, as a first priority, velocity profiles and skin friction throughout the detachment and separated regions of a (nominally) two-dimensional separating boundary layer.

The method used to produce the required flow was similar to the one reported by Chu and Young,² the details of which are given in the following section. Flow adjustment with this arrangement appears to be somewhat easier than it is with Simpson's in which a flexible tunnel roof was used. Section II also describes the measurement techniques used. The occurrence of a number of unexpected flow phenomena in the region prior to separation led to rather more measurements in that part of the flow than originally anticipated; these are discussed in Sec. III. Section IV presents some of the data obtained in the separated region and briefly discusses their implications.

II. Experimental Arrangements

A. The Wind Tunnel

The measurements were made in the no. 1 blowdown, open-circuit tunnel in the Department of Mechanical Engineering. Its working section is $0.76 \times 0.61 \times 4$ m long, and the maximum velocity is around 17 m/s. At this speed the freestream turbulence level is below 0.25%. Figure 1 shows the experimental setup used to produce the separating boundary layer. This is similar to the method used by Woodward³ who studied laminar separation bubbles. Later, Chu and Young² found this

arrangement equally effective in producing turbulent boundary-layer separation.

The apparatus consisted of three aluminum flat plates, each 1.21 m long and 10 mm thick, which spanned the 0.6 m horizontal width of the tunnel and formed the main 3.63 m surface. An elliptical-nosed section was attached to the leading edge of the plate, which was at zero incidence and about 250 mm above the floor of the tunnel. Two of the three sections of the flat plate were equipped with circular instrumentation ports positioned 200 mm apart; the third rearward section had a 0.84 m slot fitted with segmented rectangular blocks of various lengths. For each measuring instrument a special block was constructed, with a suitable hole and appropriate probe-fixing arrangements.

A porous cylinder of nominal diameter 75 mm was mounted through the sidewalls of the tunnel about 110 mm above the flat plate and normal to the flow. Its axis was parallel to the plate and about 2.7 m from its leading edge. Attached flow was maintained around the cylinder by applying suction through the porous surface. A small flap fitted to the rear of the cylinder allowed generation of the required circulation; as

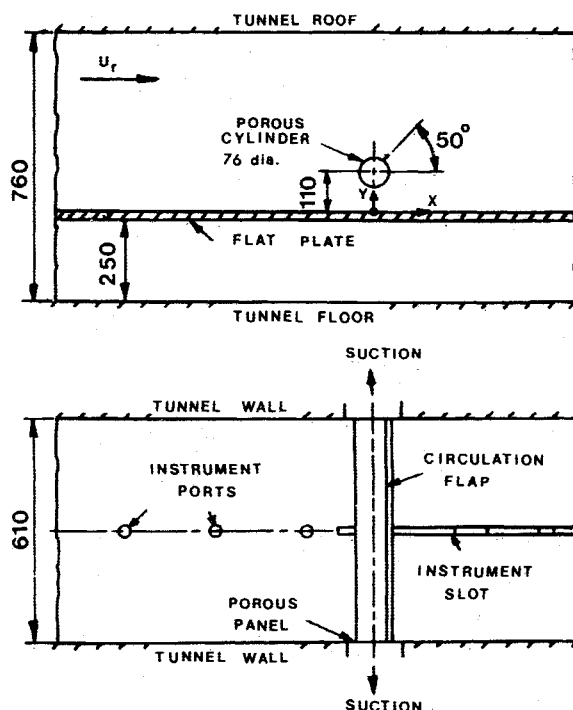


Fig. 1 Experimental arrangements (not to scale), dimensions in n.m.

Received June 22, 1987. Copyright © American Institute of Aeronautics and Astronautics, Inc., 1986. All rights reserved. AIAA regrets the long delay in publishing this paper; it was caused by a number of problems, including a large backlog of papers and a misunderstanding regarding artwork.

*Research Fellow, Department of Mechanical Engineering; currently at the Department of Chemical Engineering, Imperial College, London.

†Reader, Department of Mechanical Engineering.

the flap angle increased, more suction was required to maintain attached flow. Consequently, the pressure gradient imposed on the flat plate was initially favorable and then adverse. To prevent strong three-dimensional effects being generated by separations at the junction of the cylinder with the tunnel side-walls, the cylinder passed through porous circular discs set into the tunnel walls.

B. Measurement Techniques

For measuring the surface static pressure, 0.5-mm-diam tappings in the instrumentation ports were connected to a calibrated capacitance transducer, whose output typically was averaged over 120 s. Some of the velocities in the regions of low-turbulence level (less than 20%) were obtained using standard hot-wire anemometry and flattened pitot tubes. Preston tubes were used where appropriate for the measurement of skin friction. However, the major part of the study was undertaken using specially designed pulsed-wire wall skin friction and through-wall velocity probes, both of which were based on the time-of-flight technique originally described by Bradbury and Castro.⁴

Details of the skin-friction probe and its potential and capabilities for measurements in three-dimensional highly turbulent flows are given in Castro and Dianat⁵ and Dianat and Castro.⁶ It consists essentially of three fine wires about 2 mm long mounted parallel to each other and 0.05 mm above the surface. The sensor wires are of 5 micron tungsten and positioned 0.5 mm either side of the central, 9 micron pulsed wire. All three wires are welded to prongs mounted in a 5-mm-diam circular plug. The central wire is rapidly heated with a short electrical pulse, and the time taken for the heat tracer to reach a sensor wire is measured. A separate probe of generally similar dimensions, but with an increased spacing between the wires (1 mm), was used in regions where the wall shear stresses were comparatively high.

The through-wall velocity probe has a geometry very similar to standard pulsed-wire probes but was constructed integral with a 16 mm wall plug, so that the probe head could be traversed in and out using a micrometer beneath the surface of the plug. The pulsed wire was parallel to the surface and could be positioned between 0.025 mm and 7 mm from it, whereas the vertical sensor wires moved through small holes drilled through the surface. All wires moved together so that the overall geometry did not change with pulsed-wire location. With this arrangement the calibration of the probe was independent of the particular position of the wires.

Both the skin friction and the velocity probes could be mounted in appropriate rectangular blocks or circular disks and positioned at any desired axial station, causing negligible flow disturbance. In both cases the instruments were interfaced to Commodore PET microcomputers, allowing on-line calibration and measurement.

C. Flow Adjustment

The suction applied to the cylinder surface was maintained at a fixed level by monitoring the suction pressure at one end of the cylinder. This was typically 250 mm of water and was very close to the pressure at the other end, ensuring a good degree of suction uniformity along the cylinder span. The suction required to maintain attached flow around the cylinder was determined by inspection of tufts attached on and either side of the flap; the minimum suction for which these remained steady was taken as the required value. No noticeable change in flow characteristics was observed for stronger suction. Traverses with a hot-wire anemometer showed that the cylinder wake was very thin and of low-turbulent intensity (2% at most) at the height of the cylinder axis for the particular flap angle chosen.

There were some difficulties in obtaining the required flap angle. For an angle of, say, 35 deg, surface oil film visualization revealed the presence of a clear separation line, but later measurements with the through-wall probe showed that the

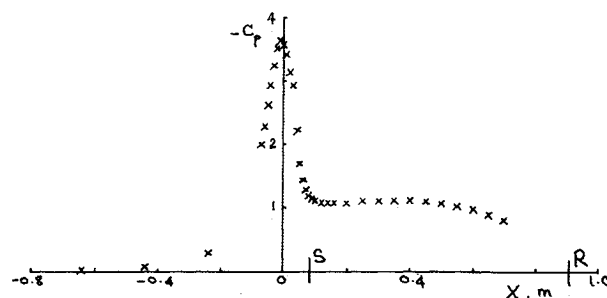


Fig. 2 Surface static pressure distribution, *S* and *R* denote the locations of separation and reattachment, respectively.

separated region was much too thin for the purposes of the present study. Rows of tufts mounted on vertical "strings" were, therefore, used downstream of the cylinder to observe the backflow region. This technique was found to be qualitatively very useful, and a flap angle of 50 deg was finally chosen as one producing an adequate fully separated boundary layer.

The two-dimensionality of the flow was investigated by traversing single hot-wire and pulsed-wire probes, where appropriate, across the span at various positions both within and outside the separated region. Careful setting up of the whole rig enabled a good degree of two-dimensionality and symmetry to be achieved over the central third of the span, with spanwise variations in mean velocity of no more than $\pm 1\%$ almost everywhere in the flow except near the separation line within the backflow region. As a further check, oil-flow visualization was undertaken in the vicinity of the separation line, which was found to be remarkably straight over practically the whole span. Just inside the backflow region, however, the flow tended to move sideways and outwards, with a weak saddle point close to the spanwise centerline.

Standard oil-flow techniques were not very successful within the bulk of the separated region where the method described by Langston and Boyle⁷ was applied. This further confirmed the two-dimensionality of the flow over the central third of the span. The position of the reattachment line was determined using the twin-tube probe described by Castro and Fackrell.⁸ It was found to be straight to within $\pm 1.5\%$ of the length of the separated region (0.83 m) over the central half of the span. Since the aspect ratio of the separated region (axial length/spanwise width) was only about 0.8, it seemed unlikely that the degree of two-dimensionality could have been significantly improved; it was thought to be quite adequate for the present purposes.

Figure 2 shows the static pressure distribution, plotted as a pressure coefficient, along the plate centerline; C_p is defined as $(p_s - p_r)/0.5\rho U_r^2$, where p_s is the surface pressure, and suffix *r* refers to freestream conditions far upstream. It may be seen that a strong adverse pressure gradient follows an initial favorable distribution. After separation at $x = 80$ mm, where x is measured from the cylinder axis position, the pressure remains nearly constant before recovering to near its upstream value farther downstream. Reattachment occurs at $x = 910$ mm. Note that neither surface pressure nor flow velocity measurements have yet been made beyond $x = 750$ mm.

III. Flow Upstream of Separation

As an initial test, skin friction was measured throughout the flow. The wall probe was calibrated against Preston tubes in the "standard" turbulent boundary layer far upstream of the cylinder (see Castro et al.⁹ or Eaton and Johnston¹⁰ for typical calibration details). The boundary layer was validated using Clauser log-law mean velocity plots, in addition to Preston tube measurements; Patel's¹¹ calibration was used for the latter.

Figure 3 shows the skin-friction distribution throughout the flow with the corresponding fluctuating data presented in Fig. 4. (Here $C_f = \tau_w/0.5\rho U_r^2$ and $c_f' = \sqrt{\tau_w^2}/0.5\rho U_r^2$). Measure-

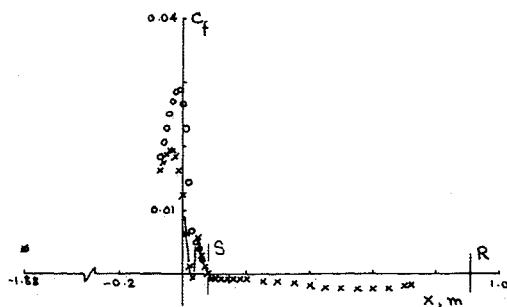


Fig. 3 Skin-friction distribution: \circ , pulsed wire; \times , Preston tube.

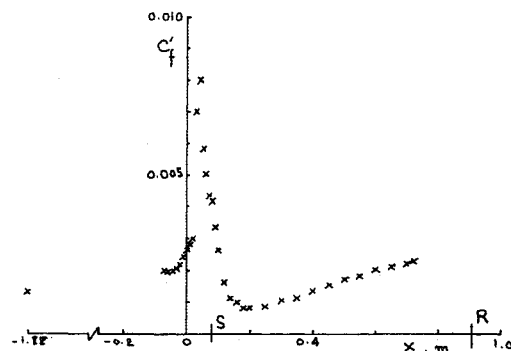


Fig. 4 Fluctuating skin-friction distribution.

ments obtained with a 1.48 mm Preston tube are included in Fig. 3. As expected, the flow experiences a continuous rise in skin friction due to the strong acceleration, followed by a sharp fall under the influence of the adverse pressure gradient. However, before the final separation, the pulsed-wire wall probe indicates a rapid rise and subsequent fall in C_f . Preston tube data give no indication of this behavior; indeed, had the pulsed-wire probe not been used, we might have been entirely satisfied with the flow: the Preston tube results are very similar to those of Chu and Young.² Closer investigation revealed that relaminarization occurred in the highly accelerated region; this persisted a short distance into the adverse pressure gradient region before transition to turbulence, with a consequent sudden rise in C_f , and finally turbulent separation at $x = 80$ mm. Note that C'_f falls to about 10% of C_f in the accelerated region, compared with its upstream value of about 30%. The latter is consistent with the near-wall data of other investigators.

Now, Kays and Crawford¹² have suggested that if the "acceleration parameter" $K = \nu/U_1^2 \cdot dU_1/dx$, where U_1 is the local freestream velocity, is maintained sufficiently large and constant along the flow, the equilibrium value of the momentum thickness Reynolds number Re_θ can be below the critical Reynolds number for transition from laminar to turbulent boundary-layer flow, in which case relaminarization takes place. A common criterion for the critical value of K is $K > 10^{-6}$, beyond which "laminar-like" behavior is observed. If K exceeds 3×10^{-6} , the entire boundary layer begins to relaminarize. This parameter is not readily available for the present experiments, but it may be estimated with reasonable accuracy from the surface pressure distribution, assuming that the pressure gradient normal to the surface is negligible. The calculation shows that K reaches a value as high as 6×10^{-6} , which is much higher than the above limit. Increasing the freestream velocity would reduce K (and increase Re_θ). However, in the present case a velocity of about 40 m/s would be required to be certain of fully turbulent flow everywhere; this was not possible for various reasons. An alternative would be to reduce dC_p/dx by reducing the flap angle, but measurements showed that, firstly, the flow ceased to separate at smaller flap angles and, secondly, even for a zero angle only a modest reduction in K (to about 4×10^{-6}) was achieved. Further, pulsed wall probe measurements showed that the charac-

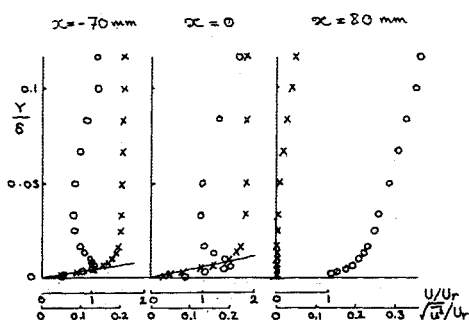


Fig. 5 Mean velocity and turbulence intensity profiles prior to separation: \times , mean velocity; \circ , intensity; —, velocity near the wall deduced from skin-friction measurements.

teristic "double hump" behavior of C_f persisted even for this reduced value of K .

Despite this initial relaminarization, it seemed likely that since the final separation was, in fact, a turbulent one, and the scale of the separated flow was so large, the nature of the latter would be largely independent of the details of the flow in the upstream region. As far as instrumentation is concerned, the fact that Preston tubes failed to capture the effects of relaminarization should be regarded as a warning against their use in nonclassical flows. Using log-law fits to velocity data would be equally uncertain in the present case.

It is interesting here to analyze the data of Chu and Young,² since they used an almost identical setup. Because of a somewhat higher freestream velocity in their experiments (20 m/s) the momentum thickness Reynolds number at the cylinder position, but in its absence, was about 4500, compared to 3000 in the present case. For the same reason, their flow experiences a somewhat milder pressure gradient. However, the maximum value of K was in excess of 2×10^{-6} —lower than the present case, but still above the critical value. There is a distinct possibility, therefore, that their flow had similar features to ours; perhaps they were not found because of instrumentation limitations. Note that in Simpson's experiments (Simpson et al.¹) K is much lower, having a maximum value of about 3×10^{-7} .

A few velocity measurements were made in the region prior to separation using the through-wall probe. This was calibrated at $x = -1.9$ m with the pulsed wire 7 mm from the surface, where the turbulent intensity (in this outer region of the local boundary layer) was about 10%. An appropriate allowance for the turbulence was made, similar to that described by Eaton and Johnston.¹⁰

Figure 5 shows the mean velocity and turbulent intensity profiles upstream of and at separation; the wall distance is normalized by the boundary-layer thickness at the position of the cylinder, but in its absence $\delta = 60$ mm. First, note that as the wall is approached the velocity data asymptote to the gradient implied by the independent skin-friction measurements. This is a satisfying confirmation of the general consistency in the measurements. Second, at $x = -70$ mm, turbulence intensities are generally low, about 13% of the mean velocity at most, confirming once again the laminar-like behavior in this region. Plots of mean velocity data in the usual wall-layer coordinates at $x = -70$ mm and $x = 0$ do not exhibit any clear linear region. This was expected—there is little reason to anticipate classic log-law behavior near separation—but emphasizes again the unsuitability of Preston tubes of any diameter.

IV. Separated Flow

The through-wall velocity probe was used in the region near the surface, whereas further away from the wall standard pulsed-wire probes and, in the lower intensity regions, single hot wires were used. Figure 6 presents longitudinal mean velocity profiles at four stations after separation, with the wall distance normalized by the centerline bubble length L_r . Corresponding turbulence intensity profiles are shown in Fig. 7.

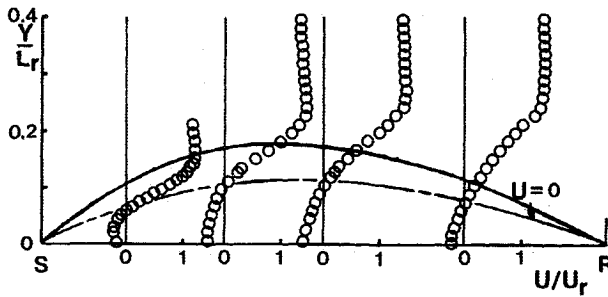


Fig. 6 Mean velocity profiles in the separated flow. Note the locus of $U = 0$.

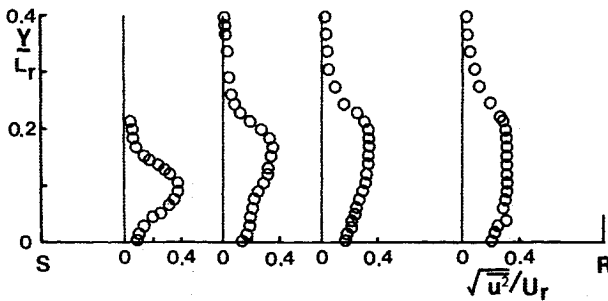


Fig. 7 Turbulent intensity profiles in the separated flow.

The growth of the shear layer is commonly measured in terms of the increase in its vorticity thickness Λ , defined by

$$\Lambda = \left| \frac{d(U/\Delta U)}{dy} \right|_{\max}^{-1}$$

where $\Delta U = U_1 - U_N$, U_1 and U_N are the maximum and minimum velocities, respectively. This is shown normalized by L_r and plotted against x'/L_r in Fig. 8; x' is the distance from the separation point ($x' = x - 80$ mm). The results of Ruderich and Fernholz¹³ (hereafter, RF) for the case of the separated region behind a normal flat plate with a long, central, downstream splitter plate are included in the figure. Because of the limited number of velocity profiles obtained thus far, it is not sensible to draw definitive conclusions, although it is interesting that the growth rate is apparently very similar to that of the classical plane mixing layer (PML), shown for comparison in the figure. However, the data of RF and some data of our own in a similar flow (Castro and Hague¹⁴) is not really consistent with a linear increase in Λ . There is little reason to suppose that the shear layer bounding the reversed flow region in the present case should grow linearly.

Figure 9 shows the development of the maximum values of u^2 , normalized by $(\Delta U)^2$. The corresponding RF data is included along with the value found in the PML. There are clear differences between these three cases, which are much more pronounced than the differences in growth rate. Indeed, the behavior in the present case is qualitatively quite different from that found by RF in the normal flat plate flow. The latter shows a continuous rise toward reattachment and a fall thereafter; the present data have the opposite behavior. This is probably caused by the unsteady nature of the separation in the present turbulent boundary-layer flow. By "unsteadiness" we mean here simply that the separation point is not fixed but fluctuates quite widely; instantaneous skin friction could take either sign over a range of axial distance spanning the time-mean $C_f = 0$ position, as has been shown by previous workers.¹ Although the entire separated shear layer may well be influenced by this general unsteadiness, the effects might be anticipated to be more obvious in the region close to separation. Note that in the RF experiment, the separation line was fixed at the sharp edge of the plate, and so no corresponding unsteadiness occurred, although in our similar experiments there was some evidence of shear layer "flapping."¹⁴

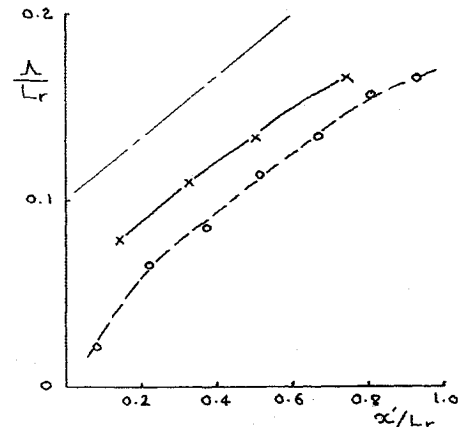


Fig. 8 Growth of the vorticity thickness: x, present work; o RF; —, PML (arbitrary virtual origin).

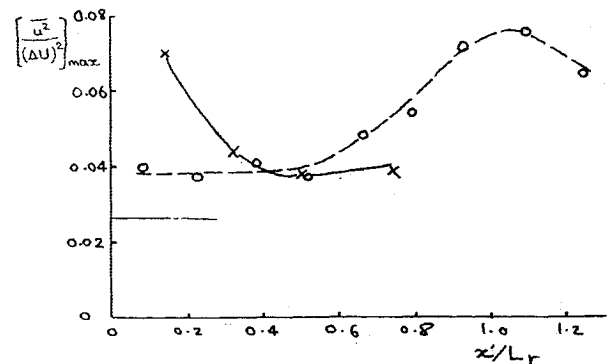


Fig. 9 Development of the maximum normal Reynolds stress (legend as in Fig. 8).

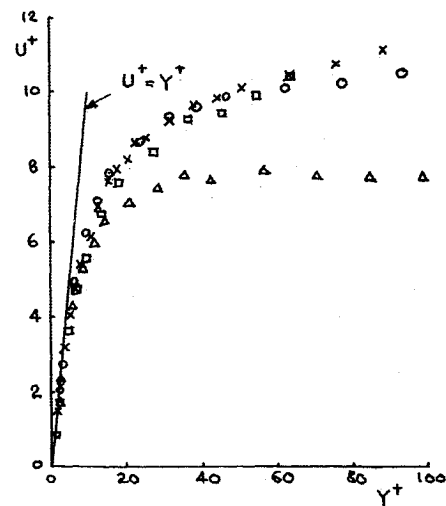


Fig. 10 Backflow near-wall velocity profiles— x'/L_r : \square , 0.145; x , 0.325; \circ , 0.506; \triangle , 0.747.

The trend in axial turbulence energy levels reverses in the region nearer the wall. This is evident from the results in Fig. 7 and is also demonstrated by the c_f data shown in Fig. 4. It may be seen that c_f is highest near the reattachment zone and decreases as the internal boundary in the separated region develops toward the separation point.

In the near-wall region, the flow must be significantly influenced by viscosity. Figure 10 presents the mean velocity data in this region plotted in the usual wall units, using the wall shear velocity implied by the skin-friction measurements. The profiles asymptote to the $U^+ = Y^+$ line for $Y^+ < 4$, again confirming the consistency of the measurements. Note, however,

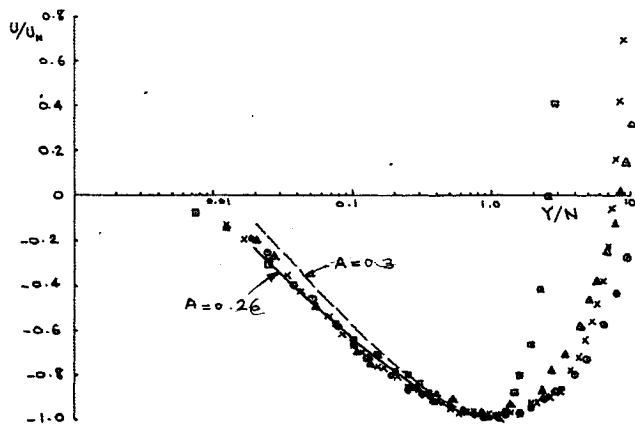


Fig. 11 Normalized backflow mean velocity profiles (legend as in Fig. 10).

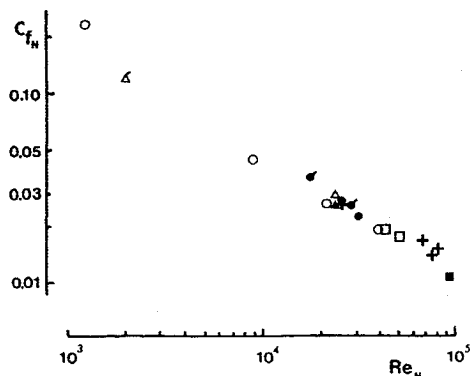


Fig. 12 Normalized wall friction within separated regions: +, present results; Δ , axisymmetric step, Davenport¹⁷; \triangle , plane back-step, Adams et al.¹⁵; \blacksquare , Chandruda and Bradshaw¹⁶; \bullet , normal flat plate, Ruderich and Fernholz¹³; \circ , \diamond , our laboratory; $Re_N = U_N(L_r - x')/\nu$, $C_{fN} = \tau_w/0.5\rho U_N^2$.

that the raw data (not shown) departs a little from this line in the sublayer region ($y^+ < 4$)—increasingly so as the wall is approached. This is due to the significant effects of diffusion in that region, which lead to a more complex heat-tracer flight path. However, it was possible to apply corrections for these effects, based on simple ideas about the flight path. These corrections were validated in standard zero pressure gradient boundary layers and will be discussed in a forthcoming paper.

The U^+ vs y^+ law-of-the-wall is not valid in the backflow region. This has been pointed out by Simpson et al.,¹ who found a good correlation when the mean velocity and distance from the wall were normalized by the maximum negative velocity U_N and its distance from the wall N , respectively. Figure 11 shows the data plotted in this form. Simpson¹⁵ suggested the use of

$$U/U_N = A[y/N - \ln(y/N) - 1] - 1 \quad (1)$$

with $A = 0.3$. In the present case, a good correlation exists for $y/N < 1$ with $A = 0.235$. The reason for this difference is not clear, and further work is needed to substantiate the existence of a "universal law"; it should be noted that Simpson's data showed considerably more scatter than is present in the results shown in Fig. 10.

The fact that this is a viscosity-dominated region suggests the possibility of correlation between the friction coefficient and the Reynolds number if these are appropriately defined. Ignoring for the moment the highly turbulent nature of the backflow, one appropriate Reynolds number for the boundary layer developing underneath it is that based on the distance from the reattachment point and the minimum (negative) velocity U_N . Figure 12 shows the values of surface skin friction,

also normalized by U_N , plotted against this Reynolds number. Additional data is shown for backward-facing step flows) Adams et al.,¹⁶ Chandruda and Bradshaw,¹⁷ and Devenport¹⁸) and for the RF flat plate flow, along with some results obtained in our laboratory, also in a normal flat plate flow. The data from all geometries collapse remarkably well. They also lie on a line having a slope of about -0.5 , consistent with the idea that the boundary layer has strong laminar-like features (see also Adams et al.¹⁶). However, we recognize that description of the flow in this region as being essentially laminar is far too simplistic, although there is no doubt that it must be dominated by viscous effects. Perhaps the outer backflow is of such a relatively large scale that it simply acts as a "quasisteady" outer boundary condition.

V. Conclusions

Through effective use of pulsed-wire anemometry some new information about separating flows has been obtained. The major conclusions from this first phase of the work can be summarized as follows:

1) A separated shear layer bounding a highly turbulent reversed-flow region has features quite different from those of the classical plane mixing layer. It seems further that these differences depend on the nature of the initial separation process.

2) The backflow mean velocity profile scales on the maximum negative mean velocity U_N and its distance from the wall N for $y/N < 1$, but the data differ somewhat from those of Simpson,¹⁵ which were obtained in the separated flow following a rather milder adverse pressure gradient.

3) The flow close to the wall in the backflow region is strongly influenced by viscosity. Not only has the linear sublayer been experimentally confirmed for $y^+ < 4$, but it seems that a universal collapse of skin-friction data from separated flows of quite different geometry may be possible.

Finally, it should be emphasized that the work described here forms just the first phase of an extensive investigation of separated boundary-layer flows. We are currently undertaking a wide range of more detailed turbulence measurements, with the intention of making further comparisons between different kinds of separated flows and hence, we hope, developing a deeper understanding of the reasons for differences between them.

Acknowledgments

The financial support of the Procurement Executive, Ministry of Defence, and the Science and Engineering Research Council is gratefully acknowledged. The work would not have been possible without the technical skill of Mr. T. Laws in development of the pulsed-wire probes.

References

- Simpson, R. L., Chew, Y. T., and Shivaprasad, B. G., "The Structure of a Separating Turbulent Boundary Layer. Part I: Mean Flow and Reynolds Stresses," *Journal of Fluid Mechanics*, Vol. 113, 1981, pp. 23-51.
- Chu, J. and Young, A. D., "Measurements in Separating Two-Dimensional Turbulent Boundary Layers," AGARD CP-168, Paper 13, 1976.
- Woodward, D. S., "An Investigation of the Flow in Separation Bubbles," Ph.D. Thesis, Queen Mary College, London, 1970.
- Bradbury, L. J. S. and Castro, I. P., "A Pulsed Wire Technique for Velocity Measurements in Highly Turbulent Flows," *Journal of Fluid Mechanics*, Vol. 49, 1971, pp. 657-691.
- Castro, I. P. and Dianat, M., "Surface Flow Patterns on Rectangular Bodies in Thick Boundary Layers," *Journal of Wind Engineering and Industrial Aerodynamics*, Vol. 11, 1983, pp. 107-119.
- Dianat, M. and Castro, I. P., "Fluctuating Surface Shear Stresses on Bluff Bodies," *Journal of Wind Engineering and Industrial Aerodynamics*, Vol. 17, 1984, pp. 133-146.
- Langston, L. S. and Boyle, M. T., "A New Surface Streamline Flow Visualization Technique," *Journal of Fluid Mechanics*, Vol. 125, 1982, p. 53.

⁸Castro, I. P. and Fackrell, J. E., "A Note on Two-Dimensional Fence Flows with Emphasis on Wall Constraint," *Journal of Industrial Aerodynamics*, Vol. 3, 1978, pp. 1-20.

⁹Castro, I. P., Dianat, M., and Bradbury, L. J. S., "The Measurement of Fluctuating Skin Friction with a Pulsed Wire Probe," *Turbulent Shear Flows V*, edited by Durst et al., Springer-Verlag, 1987, pp. 278-290.

¹⁰Eaton, J. K. and Johnston, J. P., "Turbulent Flow Reattachment: An Experimental Study of the Flow Structure Behind a Backward Facing Step," Thermosciences Div., Dept. of Mechanical Engineering, Stanford Univ., Stanford, CA, Rept. MD-39, 1980.

¹¹Patel, V. C., "Calibration of the Preston Tube and Limitations on its Use in Pressure Gradients," *Journal of Fluid Mechanics*, Vol. 23, 1965, pp. 185-208.

¹²Kays, W. M. and Crawford, M. E., *Convective Heat and Mass Transfer*, McGraw-Hill, New York, 1980, pp. 178-179.

¹³Ruderich, R. and Fernholz, H. H., "An Experimental Investiga-

tion of a Turbulent Shear Flow with Separation, Reverse Flow, and Reattachment," *Journal of Fluid Mechanics*, Vol. 163, 1986, pp. 283-322.

¹⁴Castro, I. P. and Haque, A., "The Structure of a Turbulent Shear Layer Bounding a Separation Region," *Journal of Fluid Mechanics*, Vol. 179, 1988, pp. 439-468.

¹⁵Simpson, R. L., "A Model for the Backflow Mean Velocity Profile," *AIAA Journal*, Vol. 21, 1983, pp. 142-143.

¹⁶Adams, E. W., Johnston, J. P., and Eaton, J. K., "Experiments on the Structure of a Turbulent Reattaching Shear Layer," Thermosciences Div., Dept. of Mechanical Engineering, Stanford Univ., Stanford, CA, Rept. MD-43, 1984.

¹⁷Chandrsuda, C. and Bradshaw, P., "Turbulent Structure of a Reattaching Mixing Layer," *Journal of Fluid Mechanics*, Vol. 110, 1981, pp. 171-194.

¹⁸Devenport, W. J., "Separation Bubbles at High Reynolds Number: Measurement and Computation," Ph.D Thesis, Cambridge Univ., Cambridge, MA, 1985.

*Recommended Reading from the AIAA
Progress in Astronautics and Aeronautics Series . . .*



Monitoring Earth's Ocean, Land and Atmosphere from Space: Sensors, Systems, and Applications

Abraham Schnapf, editor

This comprehensive survey presents previously unpublished material on past, present, and future remote-sensing projects throughout the world. Chapters examine technical and other aspects of seminal satellite projects, such as Tiros/NOAA, NIMBUS, DMS, LANDSAT, Seasat, TOPEX, and GEOSAT, and remote-sensing programs from other countries. The book offers analysis of future NOAA requirements, spaceborne active laser sensors, and multidisciplinary Earth observation from space platforms.

TO ORDER: Write AIAA Order Department,
370 L'Enfant Promenade, S.W., Washington, DC 20024

Please include postage and handling fee of \$4.50 with all orders.
California and D.C. residents must add 6% sales tax. All foreign orders
must be prepaid. Please allow 4-6 weeks for delivery. Prices are subject
to change without notice.

1985 830 pp., illus. Hardback

ISBN 0-915928-98-1

AIAA Members \$59.95

Nonmembers \$99.95

Order Number V-97